

COMPUTATIONAL METHODS FOR ACID MINE DRAINAGE MANAGEMENT: SIMULATION OF HYDROGEOCHEMICAL PROCESSES IN ABANDONED UNDERGROUND COAL MINES¹

Natalie A.S. Kruse², Paul L. Younger², and Vedrana Kutija²

Abstract. Predicting post-mining water quality is a key task in managing mine drainage. The most scientifically-defensible approach would be to undertake thermodynamics-based modeling of coupled geochemical and hydrodynamic processes occurring in flooded and partly flooded underground workings. Most models currently in use make the fatal assumption of local equilibrium, or else do not include all important geochemical and geometrical components of an abandoned mine system. Hydrologic and geochemical data have been incorporated into a model (Pollutant Sources & Sinks in Underground Mines) that models one-dimensional reactive transport along a mine roadway. POSSUM is an object-oriented program that models the evolution of mine water quality, accounting for contaminant sources and sinks, water level changes (due to rebound and seasonal fluctuations), reaction kinetics, variable flow regimes, infiltration through porous media, and inflow from secondary roadways. The main metals included in POSSUM's analysis are Fe, Al, Mn, Ni, and Zn. Additionally, carbonates, including limestone, ankerite and siderite, and silicates, including K-feldspar, anorthite, albite and muscovite are represented in POSSUM. Reversible sorption is also accounted for. Contaminant transport is solved using the NOAH 1-D program developed at University of Newcastle. POSSUM solves for concentrations in both the aqueous and solid phases using sequential iterations of finite difference numerical methods. Data sets from the National Coal Mining Museum in Wakefield and Coal Authority boreholes have been collected for comparison with model results. In contrast to pre-existing models, POSSUM couples kinetically controlled multi-component reactions with variable transport and will further the 'state of the art' by improving the defensibility of predictions of water quality changes over time.

Additional Key Words: reactive transport modeling, object-oriented programming, random walk method

¹ Paper presented at the 7th International Conference on Acid Rock Drainage (ICARD), March 26-30, 2006, St. Louis MO. R.I. Barnhisel (ed.) Published by the American Society of Mining and Reclamation (ASMR), 3134 Montavesta Road, Lexington, KY 40502

²Natalie A.S. Kruse, Ph.D. Student, Institute for Research in Environment and Sustainability, University of Newcastle, Newcastle upon Tyne, NE1 7RU, United Kingdom. Paul L. Younger, Professor, Institute for Research in Environment and Sustainability, University of Newcastle, Newcastle upon Tyne, NE1 7RU, United Kingdom. Vedrana Kutija, Lecturer, School of Civil Engineering and Geosciences, University of Newcastle, Newcastle upon Tyne, NE1 7RU, United Kingdom.

7th International Conference on Acid Rock Drainage, 2006 pp 966-974

DOI: 10.21000/JASMR06020966

<https://doi.org/10.21000/JASMR06020996>

Introduction

Once present in the water column, predicting the geochemical transformations and transport of contaminants are important steps in managing abandoned mine lands. This may be done using computer models; however, many current models have overlooked necessary components for accurate prediction of acid mine drainage. The computational tools available today have some specific drawbacks:

- No methods for simultaneously solving for hydraulic and geochemical changes;
- Few methods for solving based on chemical kinetics;
- No specific methods for including acid generating salts in simulations;
- No specific methods for including dispersed drippers simulations;
- Catchment-wide geologic and hydraulic assumptions increases error (Birkinshaw et al. 2005).

The goal of this study is to overcome the aforementioned problems of currently used reactive transport models. This will be incorporated into an object-oriented model, Pollutant Sources & Sinks in Underground Mines (POSSUM). POSSUM includes about 30 reactions to describe pollutant sources and sinks in underground mine systems; each of these reactions is described by either a published or thermodynamically calculated rate law. The chemical model is coupled with the Newcastle Object-oriented Appplied Hydraulics (NOAH) model which solves for flow and depth of water over time and along the flow path. Object-oriented programming is used to allow for a more robust and adaptable solution tool than traditional procedural programming would provide. This paper describes and discusses the model design and preliminary results.

Considerations for the Conceptual Model

A flooded underground mine is a complex and dynamic geochemical and hydraulic system. In order to accurately represent the hydro-geochemical system in a computational model, the reactions and hydrologic conditions considered must be chosen with care. The following sections describe the basis for the conceptual model that led to the creation of POSSUM. The set of governing geochemical reactions included in the POSSUM model are shown in Table 1.

Geochemical Conditions and Assumptions

One of the primary research questions relates to the kinetics of acid mine drainage production. Many studies have tried to quantify rates of reaction for weathering of pyrite and other related sulfides with varying degrees of success (e.g. Sung and Morgan 1980, Wiersma and Rimstidt 1984, McKibben and Barnes 1986, Nicholson et al. 1988, Elberling et al. 1993, Rimstidt and Newcomb 1993, Williamson and Rimstidt 1994, Stromberg and Banwart 1999, Holmes and Crundwell 2000, Malmström et al. 2000, Brown and Glynn 2003, Roden 2004). In order to create a realistic reactive transport model, a single set of applicable reaction rates should be used. Since conducting independent experiments to determine rates that are already available is out of the scope of this research, reaction rates from existing literature will be used, with appropriate ‘scaling’ from lab to field values (where applicable) using the approach of Malmstrom et.al. (2000). This scaling method uses calculated scaling coefficients to account for differences in particle surface area, pH, and temperature.

Table 1. Geochemical reactions represented within the POSSUM model.

Process	Reaction
Pyrite Oxidation	$\text{FeS}_{2(s)} + \text{H}_2\text{O} + 7/2\text{O}_{2(aq)} \rightarrow \text{Fe}^{2+} + 2\text{SO}_4^{2-} + 2\text{H}^+$
	$\text{FeS}_{2(s)} + 8\text{H}_2\text{O} + 14\text{Fe}^{3+} \rightarrow \text{Fe}^{2+} + 2\text{SO}_4^{2-} + 2\text{H}^+$
Chalcopyrite Oxidation	$\text{CuFeS}_{2(s)} + 4\text{O}_{2(aq)} \rightarrow \text{Fe}^{2+} + 2\text{SO}_4^{2-} + \text{Cu}^{2+}$
	$\text{CuFeS}_{2(s)} + 16\text{Fe}^{3+} + 8\text{H}_2\text{O}_{(aq)} \rightarrow 17\text{Fe}^{2+} + 2\text{SO}_4^{2-} + \text{Cu}^{2+} + 16\text{H}^+$
Sphalerite Oxidation	$\text{ZnS}_{(s)} + 2\text{O}_{2(aq)} \rightarrow \text{Zn}^{2+} + \text{SO}_4^{2-}$
	$\text{ZnS}_{(s)} + 8\text{Fe}^{3+} + 4\text{H}_2\text{O} \rightarrow \text{Zn}^{2+} + \text{SO}_4^{2-} + 8\text{Fe}^{2+} + 8\text{H}^+$
Ferris Iron Oxidation	$\text{Fe}^{2+} + 1/4\text{O}_{2(aq)} + \text{H}^+ \rightarrow \text{Fe}^{3+} + 1/2\text{H}_2\text{O}$
Ferric Hydroxide Precipitation	$\text{Fe}^{3+} + 3\text{H}_2\text{O} \rightarrow \text{Fe}(\text{OH})_3 + 3\text{H}^+$
Millerite	$\text{NiS} + 2\text{O}_2 \rightarrow \text{Ni}^{2+} + \text{SO}_4^{2-}$
Gibbsite	$\text{Al}(\text{OH})_3 + 3\text{H}^+ \leftrightarrow \text{Al}^{3+} + 2\text{H}_2\text{O}$
Chalcocite	$\text{Cu}_2\text{S} + 2\text{O}_2 \rightarrow 2\text{Cu}^{2+} + \text{SO}_4^{2-}$
Covellite	$\text{CuS} + 2\text{O}_2 \rightarrow \text{Cu}^{2+} + \text{SO}_4^{2-}$
Pyrolusite	$\text{MnO}_2 + 2\text{H}^+ \rightarrow \text{Mn}^{2+} + 1/2\text{O}_2 + \text{H}_2\text{O}$
Pyrochroite	$\text{MnOOH} + 2\text{H}^+ \rightarrow \text{Mn}^{2+} + 1/4\text{O}_2 + 3/2\text{H}_2\text{O}$
Rhodocrosite	$\text{MnCO}_3 \leftrightarrow \text{Mn}^{2+} + \text{CO}_3^{2-}$
Goethite	$\text{FeOOH} + 3\text{H}^+ \leftrightarrow \text{Fe}^{3+} + 2\text{H}_2\text{O}$
Muscovite	$2\text{KAl}_3\text{O}_8 + 2\text{H}_2\text{CO}_3 + \text{H}_2\text{O} \rightarrow \text{Al}_2\text{S}_2\text{O}_5(\text{OH})_4 + 4\text{SiO}_2 + 2\text{K}^+ + 2\text{HCO}_3^-$
K-Feldspar	$\text{KAlSi}_3\text{O}_8 + \text{H}^+ + 9/2\text{H}_2\text{O} \rightarrow 2\text{H}_4\text{SiO}_4 + 1/2\text{Al}_2\text{Si}_2\text{O}_5(\text{OH})_4$
Albite	$\text{CaAl}_2\text{Si}_2\text{O}_8 + 2\text{H}^+ + \text{H}_2\text{O} \rightarrow \text{Ca}^{2+} + 2\text{H}_4\text{Si}_4 + 1/2\text{Al}_2\text{Si}_2\text{O}_5(\text{OH})_4$
Anorthite	$\text{NaAlSi}_3\text{O}_8 + \text{H}^+ + 9/2\text{H}_2\text{O} \rightarrow \text{Na}^+ + 2\text{H}_4\text{SiO}_4 + 1/2\text{Al}_2\text{Si}_2\text{O}_5(\text{OH})_4$
Kaolinite	$\text{Al}_2\text{Si}_2\text{O}_5(\text{OH})_4 + 6\text{H}^+ \leftrightarrow 2\text{Al}^{3+} + 2\text{Si}(\text{OH})_4 + \text{H}_2\text{O}$
Calcite	$\text{CaCO}_3 \leftrightarrow \text{Ca}^{2+} + \text{CO}_3^{2-}$
Aragonite	$\text{CaCO}_3 \leftrightarrow \text{Ca}^{2+} + \text{CO}_3^{2-}$
Dolomite	$\text{CaMg}(\text{CO}_3)_2 \leftrightarrow \text{Ca}^{2+} + \text{Mg}^{2+} + 2\text{CO}_3^{2-}$
Ferric Hydroxide Dissolution	$\text{Fe}(\text{OH})_3 + 3\text{H}^+ \leftrightarrow \text{Fe}^{3+} + 3\text{H}_2\text{O}$
Gypsum	$\text{CaSO}_4 \cdot \text{H}_2\text{O} \leftrightarrow \text{Ca}^{2+} + \text{SO}_4^{2-} + \text{H}_2\text{O}$
Siderite Dissolution (crystalline)	$\text{FeCO}_3 \leftrightarrow \text{Fe}^{2+} + \text{CO}_3^{2-}$
Siderite Dissolution (precipitated)	$\text{FeCO}_3 \leftrightarrow \text{Fe}^{2+} + \text{CO}_3^{2-}$
Siderite Weathering	$\text{FeCO}_3 + \text{H}^+ \rightarrow \text{Fe}^{2+} + \text{HCO}_3^-$
Ankerite	$\text{Ca}(\text{Mg,Fe})(\text{CO}_3)_2 \rightarrow \text{Ca}^{2+} + 0.5\text{Mg}^{2+} + 0.5\text{Fe}^{2+} + 2\text{HCO}_3^-$
Anhydrite	$\text{CaSO}_4 \leftrightarrow \text{Ca}^{2+} + \text{SO}_4^{2-}$
Brucite	$\text{Mg}(\text{OH})_2 + 2\text{H}^+ \leftrightarrow \text{Mg}^{2+} + 2\text{H}_2\text{O}$
Boehmite	$\text{AlOOH} + 3\text{H}^+ \leftrightarrow \text{Al}^{3+} + 2\text{H}_2\text{O}$
Strontianite	$\text{SrCO}_3 \leftrightarrow \text{Sr}^{2+} + \text{CO}_3^{2-}$
Celestite	$\text{SrSO}_4 \leftrightarrow \text{Sr}^{2+} + \text{SO}_4^{2-}$
Barite	$\text{BaSO}_4 \leftrightarrow \text{Ba}^{2+} + \text{SO}_4^{2-}$
Magnesium Sulphate	$\text{Mg}^{2+} + \text{SO}_4^{2-} \leftrightarrow \text{MgSO}_4$
Smithsonite	$\text{ZnCO}_3 \leftrightarrow \text{Zn}^{2+} + \text{CO}_3^{2-}$

Rate Law Determination. Many lab-determined rate expressions have been developed for the weathering of pyrite. Reviews of pyrite weathering rate expressions are also available (Evangelou and Zhang 1995, Holmes and Crundwell 2000, Banwart et al. 2002, Blowes et al. 2003, Brantley 2003). The selected rate law for weathering of pyrite has been chosen for the consistency of results at field sites in Northern England (Salmon 2003). Where rate expressions are not available in the literature, thermodynamics have been used for rate approximation within the POSSUM model. Table 2 presents the major reaction rates used for geochemical calculations in the POSSUM model. These reactions include oxidation of pyrite, chalcopyrite and sphalerite by both O_2 and Fe^{+3} Fe; weathering of chlorite, muscovite, and plagioclase; Fe^{+2} Fe oxidation to Fe^{+3} Fe; and dissolution of dolomite and calcite.

Although the kinetic expressions used in the model are central to an accurate result, these are easily modified within the object-oriented code. Each of the rate laws used in the current version of POSSUM were chosen for their consistency when compared with field data collected from several sites studied by the University of Newcastle Upon Tyne.

Hydraulic Conditions and Assumptions

Deep mining activities almost invariably allow for movement of mine water post-closure due to the maintenance of underground roadways, shafts, adits, etc. for the movement of miners, mined material, waste rock, equipment and ventilation. When dewatering efforts cease after mine closure, groundwater rebound will follow. The mine workings and surrounding strata will gradually flood until the water reaches a ‘decant point’ where it may spill over, generally into surface watercourses. These points are often man-made features such as shafts and drifts. If the strata surrounding the mine workings contain sulfide minerals, the discharging waters may be highly polluted and cause massive degradation of surface and groundwater quality. The first flush of water from mine voids during groundwater rebound may be highly toxic due to the sudden release of dissolved acid generating salts from large areas of formerly dewatered mine workings (Younger 1993, Sherwood and Younger 1994, 1997, Younger 1998, Adams and Younger 2000, 2001, 2002, Younger et al. 2002).

Biological Effects

The production of acid mine drainage is catalyzed by micro organisms. These are chemolithotrophs that metabolize Fe and sulfide in the presence of O_2 . Several types of bacteria in the genera *Thiobacillus*, *Leptospirillum*, and *Sulfobacillus* have been implicated. *Acidithiobacillus ferrooxidans* can metabolize Fe^{+2} Fe, elemental S and sulfide minerals; the optimum pH range for growth is 2.0 to 2.5, but *A. ferrooxidans* can tolerate pH between 1.5 and 6.0. *Leptospirillum ferrooxidans* is similar to *A. ferrooxidans* but thrives in the pH range 1.5 to 2.1 (Blowes et al. 2003). Two mechanisms of oxidation are generally considered plausible—a direct contact mechanism and an indirect mechanism. The direct contact mechanism is defined as pyrite oxidation due to the adsorption of the bacteria directly to the surface of the mineral. The indirect mechanism, however, acts through the bacteria providing high concentrations of ferric Fe at the mineral surface and these ions oxidizing the pyrite (Lundgren et al. 1972, Boon et al. 1998, Blowes et al. 2003).

Table 2. Rate expressions for secondary geochemical reactions.

Process	Rate Expression	Constants	Reference
Pyrite oxidation (by oxygen)	$r = k[O_2]^{0.5}[H^+]^{-0.11}$	$k = 8.7 \times 10^{-12}$	(Salmon 2003)
Pyrite oxidation (by ferric Fe)	$r = k[Fe^{3+}]^{0.62}$	$k = 8.1 \times 10^{-10}$	(Salmon 2003)
Chalcopyrite oxidation (by oxygen)	$r = k[O_2]^{0.5}$	$k = 4.0 \times 10^{-13}$	(Salmon 2003)
Chalcopyrite oxidation (by ferric Fe)	$r = k[Fe^{3+}]^{0.43}$	$k = 1.2 \times 10^{-11}$	(Salmon 2003)
Sphalerite oxidation (by oxygen)	$r = k[O_2]^{0.5}$	$k = 5.4 \times 10^{-14}$	(Salmon 2003)
Sphalerite oxidation (by ferric Fe)	$r = k[Fe^{3+}]^{0.58}$	$k = 3.9 \times 10^{-10}$	(Salmon 2003)
Chlorite weathering	$r = k_1[H^+]^{0.5} + k_2$	$k_1 = 2.6 \times 10^{-13}$ $k_2 = 4.6 \times 10^{-15}$	(Salmon 2003)
Muscovite weathering	$r = k_1[H^+]^{0.4} + k_2$	$k_1 = 2.9 \times 10^{-14}$ $k_2 = 3.6 \times 10^{-16}$	(Salmon 2003)
Plagioclase weathering (75% Na; 25% Ca)	$r = k_1[H^+]^{0.45} + k_2$	$k_1 = 6.1 \times 10^{-14}$ $k_2 = 6.5 \times 10^{-16}$	(Salmon 2003)
Ferrous Fe Oxidation	$r = [O_2](k_1[Fe^{2+}] + k_2[FeOH^+] + k_3[Fe(OH)_2])$	$k_1 = 6.8 \times 10^{-6}$ $k_2 = 2.1 \times 10^1$ $k_3 = 6.8 \times 10^6$	(Salmon 2003)
Dolomite Dissolution	$r_{net} = k_1 a_{H^+}^n + k_2 a_{H_2CO_3^*}^n + k_3 a_{H_2O} - k_4 a_{HCO_3^-}$	$\log k_1 = 2.12 - 1880/T$ $\log k_2 = -0.01 - 1800/T$ $\log k_3 = 0.53 - 2700/T$ $\log k_4 = 3.16 - 2300/T$ $n = 0.50 \text{ to } 0.75$	(Brantley 2003)
Calcite Dissolution	$r_{net} = k_1 a_{H^+} + k_2 a_{H_2CO_3^*} + k_3 a_{H_2O} - k_4 a_{Ca^{2+}} a_{HCO_3^-}$	$\log k_1 = 0.198 - 444/T$ $\log k_2 = 2.84 - 2177/T$ $\log k_3 = -1.10 - 1737/T$ $k_4 = \frac{K_2}{K_c} \left(k_1' + \frac{1}{a_{H(s)^+}} \right) \cdot \left(k_2 a_{H_2CO_3^*(s)} + k_3 a_{H_2O} \right)$ Note: K_2 = dissociation constant for bicarbonate K_c = solubility product constant for calcite k_1' = rate constant for $CaCO_3 + H^+ \rightleftharpoons Ca^{2+} + HCO_3^-$ (s) = concentrations at surface adsorption layer	(Brantley 2003)

Bacteria have a catalyzing effect on sulfide mineral oxidation by controlling mineral solubility and reactions at the mineral surfaces. The oxidation of pyrite by abiotic mechanisms is a slow process and it would not be thermodynamically likely that any significant acidity would be produced without bacterial catalysis. Singer and Stumm (1970) found a five order of magnitude increase of reaction rate with the addition of *A. ferrooxidans* from $3 \times 10^{-12} \text{ mol L}^{-1} \text{ s}^{-1}$ to about $3 \times 10^{-7} \text{ mol L}^{-1} \text{ s}^{-1}$. This is currently incorporated into POSSUM as a straight multiplier although in the future will be fine tuned through comparison of results with field data.

Computational Approach

The computational approach taken in the creation of the POSSUM model is a unique approach to geochemical modeling. Object-oriented programming is just beginning to be recognized for its applicability to geochemical modeling. The Random-Walk method has been used in POSSUM to model contaminant transport and reaction chemistry.

Object-Oriented Programming

Object-oriented programming (OOP) is a novel programming method that contrasts strongly with traditional procedural programming. OOP is based on a set of OBJECTS each belonging to a CLASS of objects. Each object class has a set of attributes and operations that may be assigned to any object within that class. The operations may also be shared among different classes and act polymorphically, that is, act differently on different object classes. Additionally, attributes and operations may be inherited between classes in a hierarchical structure. The structure of OOP allows a much stronger connection between the data structure and program behavior than in procedural programming (Rumbaugh et al. 1991).

OOP has the benefit of being much more computationally efficient than traditional programming due to inheritance and polymorphism of operations. The structure of object-oriented programs also allows for easy modification of attributes and operations after the initial model has been built. These and other features of OOP make it especially useful and efficient for geochemical and hydrological modeling applications (Gandy 2003).

Object-oriented programming was chosen for use in the POSSUM model because it creates a more robust code. Objects representing points along the flow path are created at runtime. Each of the chemical calculation point objects contains both user entered and calculated information. OOP allows greater linkage between the calculation points and the data; it also allows for a larger variety of chemical and hydraulic conditions.

Random-Walk Method

The random-walk method is used to simulate the combined effect of advection and dispersion on solute transport. Transport by advection is approximated using the particle tracking technique while the effect of dispersion is integrated by adding random displacements to the particles after the advective transport step. This is based on the assumption that particle transport is a normally distributed random variable where the dispersive transport is the deviation from the mean of the distribution (Prickett et al. 1981, Zheng and Bennett 2002, Gandy 2003).

Particle Tracking Technique. The particle tracking technique is used to simulate advective transport of contaminants. This technique models contaminant transport as the transport of particles with specific masses of the contaminant in question. The particles' velocities are equal to the mean flow velocity. The mass of each particle and the number of particles present at a specific location is used to calculate the approximate solute concentration at that location.

Sorption may be modeled as a retardant on the particle velocity and reactions may be modeled by changing the mass of contaminant represented by each particle (Zheng and Bennett 2002).

NOAH 1D

The Newcastle Object-oriented Advanced Hydroinformatics (NOAH) modeling tools include NOAH 1D and NOAH 2D. They model predominantly free-surface flows within one and two dimensional systems, respectively. NOAH 1D solves for depth of water and flow rate throughout a flow network. This solution is determined from a finite difference solution of the Saint Venant Equations. Calculations can be made for varying channel cross sections (including rectangular, circular and irregular) for simple, branched and looped networks (Murray 2003). The POSSUM model will incorporate NOAH 1D's hydraulic solutions in the calculations of reactive transport.

Model Description and Preliminary Results: POSSUM

Model Structure: Numerical Processes and Model Outputs

The Pollutant Sources and Sinks in Underground Mines (POSSUM) model consists of three main parts: hydraulics, contaminant transport and reaction chemistry. The hydraulics units are based heavily on the NOAH 1D model; a detailed description of the NOAH model can be found in Murray (2003). The results for depth of flow and flow rate obtained at each node over each time step are used to simultaneously solve for contaminant transport. Contaminant transport is calculated using the random-walk method. Geochemical reactions including reversible sorption, oxidation-reduction, dissolution, precipitation and hydrolysis are accounted for by dynamically altering the mass that each particle represents. The reaction functions are time dependant and attempt to mirror field reaction kinetics for accurate model results.

Within NOAH 1D, the Saint-Venant Equations are solved using finite difference methods on an offset grid. This allows for flow and flow depth calculations to be alternated at sequential time steps. Particle density and thus contaminant concentration is calculated at the flow depth nodes to incorporate the flow rate calculation from the previous calculation step. The numerical scheme used in the solution is the Abbot-Ionescu scheme (Abbott and Minns 1998, Murray 2003).

The kinetic calculations proceed in several steps. This procedure is at the heart of the POSSUM model and is fundamentally the same for each reaction in the simulation, although the method presented here is for the oxidation of pyrite by O_2 . Particles are held in a list within each calculation point. Each particle has a 'type' descriptor which that relays the chemical represented by the particle. These include O_2 , $Fe^{+3} Fe$, $Fe^{+2} Fe$, SO_4^{-2} , H, Al, Mn and OH. During each time step at each calculation point, POSSUM cycles through the items stored in the particle lists counting the number of each type of particle. Since the kinetics of pyrite oxidation is based on the O_2 gradient over time (Salmon 2003), this gradient is calculated based on the count of O_2 particles at the current and previous time steps over the length of time step. This gradient is then used to calculate the change in $Fe^{+3} Fe$. This value is stored then used to calculate the change in oxygen, sulphate, hydrogen, and $Fe^{+2} Fe$. These changes are divided by the mass stored by each particle. Since the number of particles must be an integer value, the number of particles added is rounded up. Accuracy of this solution step may be increased by increasing the number of particles (decreasing the mass of each particle), although this will increase the memory requirement and may limit the speed of simulation. Once the new particles

have been added or removed from the list, POSSUM proceeds to the transport step by which transport is calculated by the random walk method.

The model results are produced as tables and charts showing both the evolution of contaminant concentrations along the flow path at a given time and through time at a given location. Additional three-dimensional results plots illustrate the contaminant concentration development along the flow path over multiple time steps. Future model development will allow for combination of the results plots of several contaminants to observe the relationships between them.

Model Testing

The POSSUM model has been tested against a data set from an abandoned coal colliery in Yorkshire, UK. To date, only preliminary testing for a small part of the mine system has been completed; however, further testing and model verification will be completed at a later date.

Field Data. Geochemical data from the Caphouse Colliery in Yorkshire, UK have been used to test the POSSUM model. A plan dated 1791 and showing workings from 1789 to 1795 includes a shaft on the Caphouse site in West Yorkshire, UK. It is probably the oldest coal-mine shaft still in everyday use in Britain today. By 1985 the economically viable coal at Caphouse Colliery was exhausted and its conversion to a Museum began. The mined strata are part of the Coal Measures sequence (Upper Carboniferous Westphalian). Seven seams were mined during the life of Caphouse Colliery. Chemical analysis of the mine water in the secondary drift shows that it is net alkaline, ferruginous and Mn rich. SEM and XRD show CaCO₃, manganese oxide, and Fe oxy-hydroxide deposits around several feeders.

Water samples have been taken weekly from May, 2005 to August 2005 and fortnightly from September 2005 until the present. The nine sample sites within the secondary drift include three feeders, one secondary channel before confluence with the main channel and five locations along the main channel over a distance of about 100 m. Field measurements have been taken for conductivity, temperature, total dissolved solids, oxidation-reduction potential, pH and alkalinity. Lab analysis of the water samples has been done by ICP-OES and IC to measure for Cl⁻, SO₄⁻², Ca, Mn, Na, K, Fe, Mn, Al, Zn, As, Cd, Co, Cr, Cu, Ni and Pb.

Preliminary Model Testing. Initial testing of the POSSUM model has been executed using the simplified conceptual model of a branched flow system illustrated in Fig. 1. Geochemical conditions from a small part of the flow system in the Caphouse Colliery secondary drift have been used for this testing. Figure 2 shows the confluence of the secondary and primary roadways that have been used for this testing. The preliminary results of the POSSUM model, presented in Table 3, show the evolution of various water quality parameters through time and along the flow path. This simulation was used to calculate the change in chemical concentrations along the flow path in the secondary drift in Caphouse Colliery over a length of six months. Only a limited suite of geochemical components have been modeled here to shorten run time. For this simulation, each node (Fig. 1) has been numbered from one to thirteen. Nodes one to nine are in the primary flow path, while nodes ten to thirteen are in the secondary flow path; the node spacing is one metre. For time $t = 0$, the geochemical data for nodes N1, N9, and N10 are entered from field data. The initial values may be entered for the other nodes as well, but are not required. At time $t = 0$, the initial geochemical conditions are calculated for the remainder of the nodes; currently this is done using linear interpolation, although a more precise method is in development. These initial conditions are then used to model the changes in water

chemistry over a period of six months. Additional data entered by the user for this type of simulation include the following:

- Initial upstream and downstream flow rates;
- Channel cross-section type;
- As much channel geometry as possible;
- Typical hydrograph to describe typical rainfall;
- Initial upstream and downstream water chemistry;
- Percentage pyrite, calcium carbonate, sphalerite, chalcopyrite and galena in the strata;
- Approximate location of secondary roadways, feeders and, where available, their flow rates;
- Approximate volume of distributed lateral inflow (drippers).

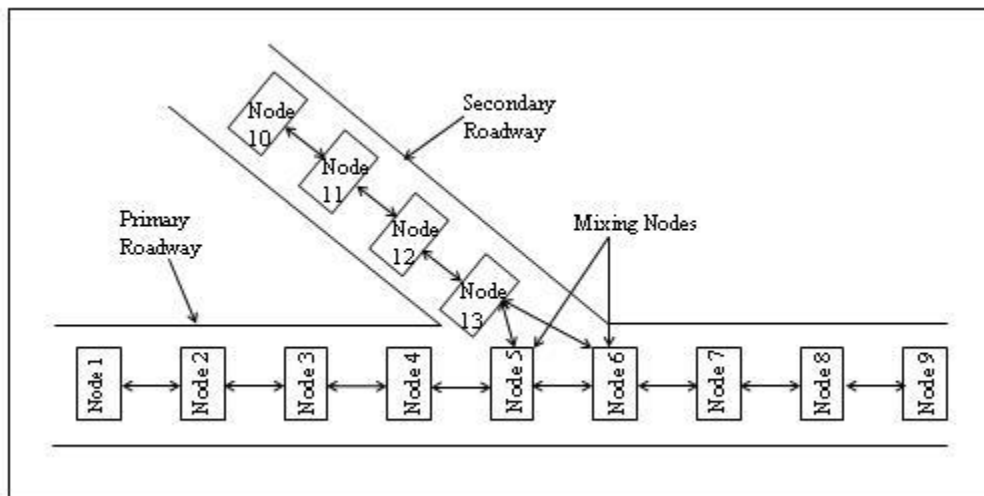


Figure 1. Simplified conceptual model for testing of POSSUM.

The results shown in Table 3 are the modeled evolution of pH, alkalinity, Cl^- , SO_4^{-2} , Ca, Fe, Mn, Al, and Zn concentrations along the flow path and through time. Initial chemical and hydraulic conditions were entered for nodes N1, N9 and N10. A linear interpolation was used to fill in the initial conditions for the remaining nodes; this is useful for sites with limited chemical data; in further model development a more accurate method for initial condition estimation will be developed. Two sets of results are presented here, one for the initial time step ($t = 0$) shown in Table 3a and one for 6 months of elapsed time ($t = 6$ months) shown in Table 3b. The fields shown in blue in Table 3 are entered by the user, while the fields shown in green are calculated by the POSSUM model as described in the previous section.



Figure 2. Confluence of primary and secondary flow paths in Caphouse Colliery used for preliminary testing of POSSUM model.

Table 3. Preliminary test results from POSSUM; concentrations in the aqueous phase.

Table 3a. Results for initial timestep. t = 0									
t=0 months									
Main Channel	pH	Alkalinity mg/L CaCO ₃	Cl ⁻ mg/L	SO ₄ ⁻² mg/L	Ca mg/L	Fe mg/L	Mn mg/L	Al mg/L	Zn mg/L
N1 (boundary)	6.73	250	101	441	167	3.5	1.5	0.17	0.02
N2	6.73	250	101	440	167	3.45	1.48	0.16	0.02
N3	6.74	265	100	439	169	3.43	1.48	0.16	0.02
N4	6.74	268	101	440	169	3.43	1.49	0.14	0.02
N5 (mixing)	7.05	299	85	370	178	2.98	1.05	0.11	0.02
N6 (mixing)	7.18	330	80	362	179	2.83	1.04	0.11	0.02
N7	7.25	341	79	361	176	2.81	1.01	0.1	0.02
N8	7.31	350	78	361	175	2.76	0.98	0.1	0.02
N9	7.5	365	76	358	172	2.7	0.93	<0.1	0.02
Secondary Channel	pH	Alkalinity mg/L CaCO ₃	Cl ⁻ mg/L	SO ₄ ⁻² mg/L	Ca mg/L	Fe mg/L	Mn mg/L	Al mg/L	Zn mg/L
N10 (boundary)	7.92	385	69	334	183	0.38	0.43	0.1	<0.01
N11	7.91	387	70	331	185	0.37	0.41	0.1	<0.01
N12	7.92	385	69	330	183	0.37	0.42	0.1	<0.01
N13	7.92	386	71	330	184	0.36	0.42	0.1	<0.01

Table 3b. Results for 6 months of elapsed time. t = 6 months									
t=6 months									
Main Channel	pH	Alkalinity mg/L CaCO ₃	Cl ⁻ mg/L	SO ₄ ⁻² mg/L	Ca mg/L	Fe mg/L	Mn mg/L	Al mg/L	Zn mg/L
N1 (boundary)	6.76	258	100	445	171	4.0	1.9	0.20	0.03
N2	6.79	261	101	450	171	3.9	1.9	0.18	0.03
N3	6.79	263	102	450	175	3.9	1.95	0.18	0.02
N4	6.81	263	100	452	176	3.85	1.88	0.17	0.02
N5 (mixing)	7.55	361	84	395	181	3.1	1.2	0.12	0.02
N6 (mixing)	7.62	365	83	393	184	3	1.19	0.11	0.02
N7	7.7	364	81	393	186	2.9	1.19	0.11	0.02
N8	7.7	364	79	392	186	2.95	1.17	0.1	0.02
N9	7.71	368	78	393	187	2.9	1.17	0.1	0.02
Secondary Channel	pH	Alkalinity mg/L CaCO ₃	Cl ⁻ mg/L	SO ₄ ⁻² mg/L	Ca mg/L	Fe mg/L	Mn mg/L	Al mg/L	Zn mg/L
N10 (boundary)	7.95	384	70	345	195	0.44	0.6	0.1	<0.01
N11	7.94	385	70	348	193	0.44	0.59	0.1	<0.01
N12	7.91	384	71	345	193	0.45	0.58	0.1	<0.01
N13	7.91	384	70	344	191	0.43	0.55	0.1	<0.01

The values calculated match the collected field data within 15% difference. Due to the sparse geologic data and low numbers of particles used for this simulation, this is a positive result. Based on the first several months of sample collection from the site, the model results are consistent with the trends seen in the field, although they are not conclusive at this stage. Future simulations will be done with more detailed geologic and hydraulic information; additionally, by using a computer with increased memory, more particles may be used in the simulation which will increase accuracy of results.

Conclusions and Further Work

From initial testing, POSSUM creates realistic and applicable results for a simple conceptual model. Preliminary results are promising for POSSUM's applicability to field data, although further comparison of results is required. In order to further verify POSSUM, two field sites in the United Kingdom, Caphouse Colliery and Nenthead Adit, will be modeled in detail and results will be compared with geochemical data from the sites. The format of model results plots and tables will also be improved upon for more easily interpretable results.

Acknowledgements

We would like to acknowledge Catherine Gandy and Michael Murray for their guidance in the creation of this model and the Marshall Aid Commemoration Commission for funding my research.

Literature Cited

- Abbott, M. B., and A. W. Minns. 1998. Computational Hydraulics, 2nd Edition edition. Ashgate Publishing Company, Aldershot, UK.
- Adams, R., and P. L. Younger. 2000. Simulating groundwater rebound in a recently closed tin mine. Pages 218-228 in D. Grabala, E. Kaczkowska, P. Siwek, and J. Wrobel, editors. 7th International Mine Water Association Congress. International Mine Water Association, Ustron, Poland.
- Adams, R., and P. L. Younger. 2001. A Strategy for Modelling Ground Water Rebound in Abandoned Deep Mine Systems. *Ground Water* 39:249-261. <http://dx.doi.org/10.1111/j.1745-6584.2001.tb02306.x>.
- Adams, R., and P. L. Younger. 2002. A physically based model of rebound in South Crofty tin mine, Cornwall. Pages 89-97 in P. L. Younger and N. S. Robins, editors. *Mine Water Hydrogeology and Geochemistry*. Geological Society, London. <http://dx.doi.org/10.1144/gsl.sp.2002.198.01.06on>.
- Banwart, S. A., K. A. Evans, and S. Croxford. 2002. Predicting mineral weathering rates at field scale for mine water risk assessment. Pages 137-157 in P. L. Younger and N. S. Robins, editors. *Mine Water Hydrology and Geochemistry*. Geological Society of London, London. <http://dx.doi.org/10.1144/gsl.sp.2002.198.01.10>
- Birkinshaw, S. J., M. C. Thorne, and P. L. Younger. 2005. Reference biospheres for post-closure performance assessment: inter-comparison of SHETRAN simulations and BIOMASS results. *Journal of Radiological Protection* 25:33-49. <http://dx.doi.org/10.1088/0952-4746/25/1/0029>.
- Blowes, D. W., C. J. Ptacek, J. L. Jambor, and C. G. Weisener. 2003. The Geochemistry of Acid Mine Drainage. Pages 149-204 in H. D. Holland and K. K. Turekian, editors. *Treatise on Geochemistry*. Elsevier-Pergamon, Oxford. <http://dx.doi.org/10.1016/b0-08-043751-6/09137-4>.
- Boon, M., M. Snijder, G. S. Hansford, and J. J. Heijnen. 1998. The oxidation kinetics of Zn sulphide with *Thiobacillus ferrooxidans*. *Hydrometallurgy* 48:171-186. [http://dx.doi.org/10.1016/S0304-386X\(97\)00081-9](http://dx.doi.org/10.1016/S0304-386X(97)00081-9)
- Brantley, S. L. 2003. Reaction Kinetics of Primary Rock-forming Minerals under Ambient Conditions. Pages 73-117 in H. D. Holland and K. K. Turekian, editors. *Treatise on Geochemistry*. Elsevier Pergammon, London. <http://dx.doi.org/10.1016/B0-08-043751-6/05075-1>.
- Brown, J. G., and P. D. Glynn. 2003. Kinetic dissolution of carbonates and Mn oxides in acidic water: measurement of in situ field rates and reactive transport modeling. *Applied Geochemistry* 18:1225-1239. [http://dx.doi.org/10.1016/S0883-2927\(03\)00010-69](http://dx.doi.org/10.1016/S0883-2927(03)00010-69).
- Elberling, B., R. V. Nicholson, and D. J. David. 1993. Field Evaluation of Sulphide Oxidation Rates. *Nordic Hydrology* 24:323-338.
- Evangelou, V. P., and Y. L. Zhang. 1995. A Review - Pyrite Oxidation Mechanisms and Acid-Mine Drainage Prevention. *Critical Reviews in Environmental Science and Technology* 25:141-199. <http://dx.doi.org/10.1080/10643389509388477>.

- Gandy, C. J. 2003. Modelling Pyrite Oxidation and Pollutant Transport in Mine Wastes using an Object-Oriented Particle Tracking Code. University of Newcastle Upon Tyne, Newcastle Upon Tyne.
- Holmes, P. R., and F. K. Crundwell. 2000. The kinetics of the oxidation of pyrite by ferric ions and dissolved oxygen: an electrochemical study. *Geochimica Et Cosmochimica Acta* 64:263-274. [http://dx.doi.org/10.1016/S0016-7037\(99\)00296-3](http://dx.doi.org/10.1016/S0016-7037(99)00296-3).
- Kleinmann, R. L. P. 2000. Prediction of Water Quality at Surface Coal Mines. The National Mine Land Reclamation Center, Morgantown, West Virginia, USA.
- Lundgren, D. G., J. R. Vestal, and F. R. Tabitha. 1972. The Microbiology of Mine Drainage Pollution. *in* R. Mitchell, editor. *Water Pollution Microbiology*. Wiley.
- Malmström, M. E., G. Destouni, S. Banwart, and B. Stromberg. 2000. Resolving the Scale-Dependence of Mineral Weathering Rates. *Environmental Science & Technology* 34:1375-1378. <http://dx.doi.org/10.1021/es990682u>.
- McKibben, M. A., and H. L. Barnes. 1986. Oxidation of pyrite in low temperature acidic solutions: Rate laws and surface textures. *Geochimica Et Cosmochimica Acta* 50:1509-1520. [http://dx.doi.org/10.1016/0016-7037\(86\)90325-X](http://dx.doi.org/10.1016/0016-7037(86)90325-X).
- Murray, M. 2003. An Investigation into Object-Oriented Approaches for Hydroinformatics Tools. University of Newcastle Upon Tyne, Newcastle Upon Tyne.
- Nicholson, R. V., R. W. Gillham, and E. J. Reardon. 1988. Pyrite oxidation in carbonate-buffered solution: 1. Experimental kinetics. *Geochimica Et Cosmochimica Acta* 52:1077-1085. [http://dx.doi.org/10.1016/0016-7037\(88\)90262-1](http://dx.doi.org/10.1016/0016-7037(88)90262-1).
- Prickett, T. A., T. G. Naymik, and C. G. Lonquist. 1981. A "Random-Walk" Solute Transport Model for Selected Groundwater Quality Evaluations. *Bulletin* 65:103.
- Rimstidt, J. D., and W. D. Newcomb. 1993. Measurement and analysis of rate data: The rate of reaction of ferric iron with pyrite. *Geochimica Et Cosmochimica Acta* 57:1919-1934. [http://dx.doi.org/10.1016/0016-7037\(93\)90084-A](http://dx.doi.org/10.1016/0016-7037(93)90084-A).
- Roden, E. E. 2004. Analysis of long-term bacterial vs. chemical Fe(III) oxide reduction kinetics. *Geochimica Et Cosmochimica Acta* 68:3205-3216. <http://dx.doi.org/10.1016/j.gca.2004.03.028>.
- Rumbaugh, J., M. Blaha, W. Premerlani, F. Eddy, and W. Lorensen. 1991. Object-Oriented Modeling and Design. Prentice-Hall, Inc., Englewood Cliffs, New Jersey.
- Salmon, S. U. 2003. Geochemical Modelling of Acid Mine Drainage in Mill Tailings. KTH Land and Water Resources Engineering, Stockholm, Sweden.
- Sherwood, J. M., and P. L. Younger. 1994. Modelling Groundwater Rebound after Coalfield Closure: An Example from County Durham, UK. Pages 767-777 *in* D. J. Reddish, editor. 5th International Mine Water Congress. University of Nottingham and IMWA, Nottingham, UK.
- Sherwood, J. M., and P. L. Younger. 1997. Modelling groundwater rebound after coalfield closure. Pages 165-170 *in* C. e. al., editor. *Groundwater in the Urban Environment: Problems, Processes and Management*. Balkema, Rotterdam.

- Singer, P. C., and W. Stumm. 1970. Acid Mine Drainage: The Rate-Determining Step. *Science* 167:1121-1123. <http://dx.doi.org/10.1126/science.167.3921.1121>.
- Stromberg, B., and S. Banwart. 1999. Weathering kinetics of waste rock from the Aitik copper mine, Sweden: scale dependent rate factors and pH controls in large column experiments. *Journal of Contaminant Hydrology* 39:59-89. [http://dx.doi.org/10.1016/S0169-7722\(99\)00031-5](http://dx.doi.org/10.1016/S0169-7722(99)00031-5).
- Sung, W., and J. J. Morgan. 1980. Kinetics and Product of Ferrous Iron Oxygenation in Aqueous Systems. *Environmental Science & Technology* 14:561-568. <http://dx.doi.org/10.1021/es60165a006>.
- Wiersma, C. L., and J. D. Rimstidt. 1984. Rates of reaction of pyrite and marcasite with ferric iron at pH 2. *Geochimica Et Cosmochimica Acta* 48:85-92. [http://dx.doi.org/10.1016/0016-7037\(84\)90351-](http://dx.doi.org/10.1016/0016-7037(84)90351-).
- Williamson, M. A., and J. D. Rimstidt. 1994. The kinetics and electrochemical rate-determining step of aqueous pyrite oxidation. *Geochimica Et Cosmochimica Acta* 58:5443-5454. [https://doi.org/10.1016/0016-7037\(94\)90241-0](https://doi.org/10.1016/0016-7037(94)90241-0)
- Younger, P. L. 1993. Possible environmental impact of the closure of two collieries in County Durham. *Journal of the Institution of Water and Environmental Management* 7:521-531. <https://doi.org/10.1111/j.1747-6593.1993.tb00881.x>
- Younger, P. L. 1998. Coalfield abandonment: geochemical processes and hydrochemical products. *Energy and the Environment: Geochemistry of fossil, nuclear and renewable resources*:1-29.
- Younger, P. L., S. Banwart, and R. S. Hedin. 2002. *Mine Water: Hydrology, Pollution, Remediation*. Kluwer Academic Publishers, London.
- Zheng, C., and G. D. Bennett. 2002. *Applied Contaminant Transport Modelling*, Second edition. John Wiley and Sons, Inc., New York.